Dual-Functional Poly(3,4-ethylenedioxythiophene)/MnO_2 Nanoellipsoids for Enhancement of Neurite Outgrowth and Exocytosed Biomolecule Sensing in PC12 Cells

*Sojin Kim, Wan-Kyu Oh, Yoon Seon Jeong, and Jyongsik Jang**

Dual-functional MnO_2-decorated poly(3,4-ethylenedioxythiophene) (PEDOT/MnO_2) nanoellipsoids are fabricated for enhancement of neurite outgrowth during differentiation and real-time monitoring of PC12 cells. The PEDOT nanoellipsoids are prepared by chemical oxidation polymerization in reverse microemulsion and the MnO_2 domains on the surface of the PEDOT are formed by redox deposition. A PC12 cell is used as a model cell for neuronal differentiation. The morphology, differentiation efficiency, average neurite length, expression level of DMT1, phosphorylation of ERK1/2, and viability of PC12 cells upon the exposure of the PEDOT/MnO_2 nanoellipsoids are examined. The PEDOT/MnO_2 nanoellipsoids facilitate neurite outgrowth in proportion to the dose of the nanoellipsoids, and MnO_2 domains play a pivotal role in facilitation effects on cell differentiation. The PEDOT/MnO_2 nanoellipsoids represent low toxicity in the cells due to biocompatible PEDOT matrix. Moreover, the PEDOT/MnO_2 nanoellipsoids are further applied as a transducer material for label-free real-time monitoring of PC12 cells. The exocytosed catecholamines from living cells are successfully detected. The dual-functionalized PEDOT/MnO_2 nanoellipsoids may be used in tissue engineering related to the development and monitoring of mammalian nervous systems.

1. Introduction

The mechanisms of nerve cell development are of crucial importance in neuroscience. Therefore, the investigation of neuron development and outgrowth has received considerable attention from biomedical engineers in past decades.[1] Cell differentiation properties are strongly affected by the morphology and composition of the extracellular matrix (ECM) and by the complex interactions between external physical and chemical stimuli.[2] In particular, it has been reported that divalent metal cations, including Mn^{2+}, Mg^{2+}, Ni^{2+}, and Cu^{2+}, can enhance cell adhesion and neurite outgrowth. For example, Mn^{2+} was immobilized with the ECM, which is involved in neuronal differentiation, by activating cell adhesion molecules and controlling mechanical tension.[3] Moreover, Mn^{2+}, like nerve growth factor (NGF), promoted the differentiation of neurons through inhibition of the dividing ability of astrocytes.[4] Mn-induced cell differentiation is dependent on its interaction with the cell-surface integrin receptors and basement membrane proteins, fibronectin, and vitronectin.[4,5]

Nanomaterials can interact with biological systems at fundamental, molecular levels with high specificity.[6] By taking advantage of this unique molecular specificity, nanomaterials can interact with, stimulate, and respond to target cells and tissues in controlled ways, while minimizing undesirable effects. The application of nanomaterials in neuroscience is stuck in the early stages of development, mainly due to the complexities associated with interacting with neural cells and the mammalian nervous system. However, nanotechnology for neuroscience research is emerging because of its unique physicochemical properties.[7] Specifically, neuronal adhesion and growth, interfacing neurons at the molecular level, and functional neural regeneration are of interest to nanotechnology researchers.

Poly(3,4-ethylenedioxythiophene) (PEDOT) has been utilized by several research groups to enhance the properties of neural interfaces.[8] Recently, Martin et al. reported the synthesis of a hybrid PEDOT-neuron electrode, which exhibited enhanced electrode functionality and cell proliferation.[8b] Additionally, experiments with NGF-modified PEDOT revealed that rat pheochromocytoma PC12 cells adhered to the substrate and extended neurites on the PEDOT film.[9] PEDOT nanomaterials have been shown to improve the charge transfer characteristics of conventional metal electrodes, and biological assays have shown that cells preferentially adhere to the electrodes.[10] Neural cells are electroactive, and the functions of nervous system are based on electrical activities. As neuronal stimulation and monitoring are needed for a variety of clinical diagnostics and treatments,[11] the unique electrical properties of PEDOT nanomaterials offer great advantages for the therapeutic and/or other purposes. Furthermore, the electronic properties of PEDOT nanomaterials can

S. Kim, W.-K. Oh, Y. S. Jeong, Prof. J. Jang
World Class University (WCU)
program of Chemical Convergence for Energy & Environment (C2E2)
School of Chemical and Biological Engineering
Seoul National University
1 Gwanangno, Gwanakgu, Seoul 151-742, Korea
E-mail: jsjang@plaza.snu.ac.kr

DOI: 10.1002/adfm.201202198

be tailored to match the charge transport required for electrical cellular interfacing.[8b,8c,10] PEDOT also exhibited higher conductivity compared to polypyrrole and polyaniline, representative conducting polymers.[12] The 3,4-dioxy substitution blocks the possibility of undesired α–β(β') couplings within the polymer backbone, resulting in a high conductivity.[13] Generally, it is known that PEDOT is stable in biological condition owing to lack of undesired α–β(β') couplings.[13b] With such properties, PEDOT nanomaterials may also be expected to offer opportunities to develop biocompatible and special-purpose interfacial materials for the neural system, such as neural chips, implanted electrodes, and drug/gene vectors.[8b,c,10,14]

Here, we report the fabrication of dual-functional MnO_2-decorated PEDOT (PEDOT/MnO_2) nanoellipsoids for facilitating neurite outgrowth during differentiation and real-time cellular monitoring of live cells. The PEDOT nanoellipsoids were prepared by chemical oxidation polymerization in reverse (water-in-oil) microemulsion, and MnO_2 domains were synthesized on the surface of PEDOT by redox deposition. Rat pheochromocytoma PC12 cells were used as the model cells for neuronal differentiation. We systematically examined the morphology, ratio of differentiation, neurite length, expression level of DMT1, phosphorylation of ERK1/2, cell viability, and uptake ratio of PC12 cells upon exposure to PEDOT/MnO_2 nanoellipsoids. Moreover, the PEDOT/MnO_2 nanoellipsoids were further applied as transducer for real-time monitoring of PC12 cells. To the best of our knowledge, this is the first investigation of the facilitation of neurite outgrowth by MnO_2 nanoparticles.

2. Results and Discussion

2.1. Fabrication of MnO_2-Decorated PEDOT Nanoellipsoids

Figure 1a shows a schematic diagram of the experimental procedure. PEDOT nanoellipsoids were synthesized in reverse cylindrical micelle phases by chemical oxidation polymerization, as previously described.[15] Briefly, sodium bis(2-ethylhexyl) sulfosuccinate (AOT) formed reverse micelles in hexane, and an aqueous $FeCl_3$ solution was introduced into the AOT/hexane system. Iron cations were adsorbed on the head groups of AOT and acted as oxidizing agents for the chemical polymerization of 3,4-ethylenedioxythiophene (EDOT) monomers at the cylindrical AOT/water interface. The PEDOT nanoellipsoids were washed thoroughly with ethanol and resuspended in water. Transmission electron microscopy (TEM) images revealed uniform, ellipsoidal shaped, and dispersed PEDOT nanoellipsoids of 55-nm width and 160-nm length (Figure 1a, inset). Subsequently, the PEDOT nanoellipsoids were treated with 10 mM potassium permanganate solution ($KMnO_4$) under vigorous stirring conditions. MnO_2-decorated PEDOT (PEDOT/MnO_2) nanoellipsoids were formed by reaction between the oxidant and the reductant.[16] Afterward, the PEDOT/MnO_2 nanoellipsoids were washed with deionized (DI) water, resuspended in 0.1 M phosphate buffered saline (PBS) solution, and applied to PC12 cells to promote neuronal differentiation. Energy-dispersive X-ray (EDX) mapping image of the PEDOT/MnO_2 nanoellipsoids indicated successful incorporation of MnO_2 on the surface of the PEDOT nanoellipsoids (Figure 1a, inset; red, S; green, Mn). The green dots were mixed with red dots, indicating that the MnO_2 and PEDOT formed a hybrid structure on the surface of PEDOT nanoellipsoids.

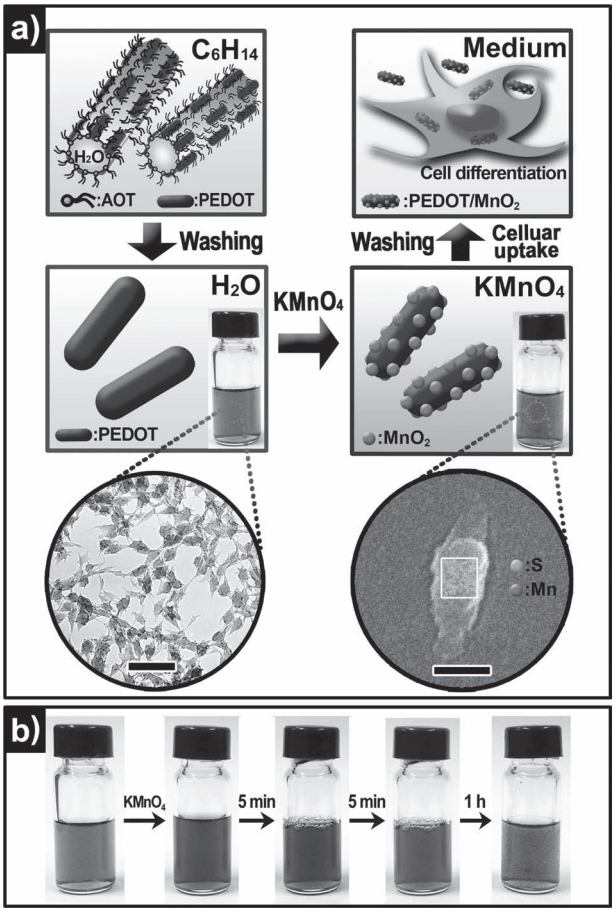

Figure 1. a) Schematic diagram of fabrication of the PEDOT/MnO_2 nanoellipsoids. Left inset: enlarged TEM image of the PEDOT nanoellipsoids. Scale bar: 200 nm. Right inset: enlarged FE-SEM image of PEDOT/MnO_2 nanoellipsoids with EDX mapping. Scale bar: 50 nm. b) Photographs of time-dependent color alteration of 10 mM $KMnO_4$-treated PEDOT nanoellipsoids.

The color of the $KMnO_4$-treated PEDOT nanoellipsoids was changed from pale blue to yellowish green as a function of time due to the formation of the brownish-colored MnO_2 (Figure 1b).[16b] Upon adding the purple $KMnO_4$, the solution immediately changed from blue to purple due to the MnO_4^- ions.[17] As MnO_2 domains grew, MnO_4^- ions in the solution were consumed, and the purple color became completely bleached, resulting in the brown color.

To confirm the presence of MnO_2 domains on the surface of PEDOT, high-resolution TEM (HRTEM) analysis was conducted. As displayed in **Figure 2**a, PEDOT/MnO_2 nanoellipsoids retained their ellipsoidal shape. The dark spots in Figure 2a,b imply the presence of MnO_2 domains and show that each domain was less than 5 nm in size. The MnO_2 domains had no lattice fringes because of the low reaction temperature,[16b] which indicates that the nature of the MnO_2 domain is amorphous. The amount of decorated MnO_2 domains on the PEDOT were calculated as

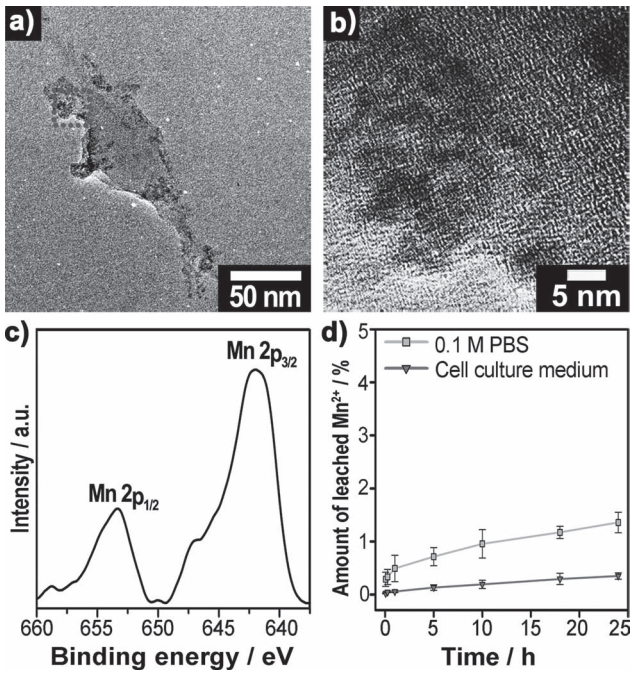

Figure 2. a) HRTEM image of PEDOT/MnO_2 nanoellipsoids and b) magnified image of boxed area in (a). c) XPS spectrum of PEDOT/MnO_2 nanoellipsoids. The PEDOT nanoellipsoids were treated with 10 mM $KMnO_4$ for 10 min. d) Leaching profile of Mn^{2+} ions from PEDOT/MnO_2 nanoellipsoids in high ionic strength solution (0.1 M PBS) and cell culture medium.

8.8 wt% by inductively coupled plasma emission spectrometer (ICP) analysis. To further clarify the oxidation state of the MnO_2 domain, X-ray photoelectron spectroscopy (XPS) analysis was conducted (Figure 2c). The peaks of Mn $2p_{3/2}$ and Mn $2p_{1/2}$ were centered at 642.0 and 653.3 eV, respectively, which is considered that most of the MnO_4^- ions in the solution were reduced to MnO_2 domains on the surface of the PEDOT matrix.[16,18]

After the formation of MnO_2 domains, the zeta potential ζ of the PEDOT/MnO_2 nanoellipsoids increased from -27.48 ± 1.85 to -30.9 ± 1.02 mV in aqueous solution because the negative surface charge of the MnO_2 domains affected on the ζ of the PEDOT/MnO_2 nanoellipsoids.[19] Dissolution of the Mn^{2+} ions was evaluated in 0.1 M PBS and cell culture medium as a function of a time (Figure 2d). A small amount of Mn^{2+} ions (0.34%) was leached in cell culture medium during 24 h incubation due to colloidal stability effects of solvents.[20]

To investigate MnO_2 formation on the PEDOT nanoellipsoids, the molecular structure of PEDOT nanoellipsoids was analyzed by XPS. The XPS spectra of S 2p can be deconvoluted into three components: sulfide (164.1 eV; blue), sulfoxide (165.1 eV; red), and sulfone bonds (168.2 eV; green) (**Figure 3**a,b).[15b,16b] The sulfoxide and sulfone bonds in pristine PEDOT nanoellipsoids were attributed to the incorporation of the sulfonate anionic head group of residual AOT surfactant, as the PEDOT nanomaterial was fabricated on the surface of AOT micelle templates.[15b] After $KMnO_4$ treatment, the sulfoxide and sulfone bonds in PEDOT/MnO_2 nanoellipsoids increased compared with those in PEDOT nanoellipsoids. It is considered that the sulfide bonds in PEDOT nanoellipsoids were transformed into sulfoxide and sulfone bonds during the $KMnO_4$ treatment. These results were confirmed by Fourier transform infrared spectroscopy (FT-IR) spectra of PEDOT nanoellipsoids treated with different concentrations of $KMnO_4$ (Figure 3c). Characteristic peaks, including S=O stretching bond at 1054 cm^{-1} and O=S=O scissoring vibration at 570 cm^{-1}, appeared and became obvious as the concentration of $KMnO_4$ increased.[16b,21] These results indicated that the sulfide bonds of the PEDOT nanoellipsoids became oxidized into sulfoxide or sulfone as the treatment time and concentration increased. Furthermore, sulfur on the thiophene ring served as a site for $KMnO_4$ reduction, and MnO_2 domains were generated simultaneously (Figure 3d).[16b] We analyzed the atomic ratio of Mn to S of the PEDOT and PEDOT/MnO_2 nanoellipsoids (**Table 1**). The atomic ratio of Mn/S increased with escalating concentration and treatment time of $KMnO_4$. It is believed that the direct-contact reaction between $MnO4^-$ and PEDOT nanoellipsoids leads to initial formation of the first nuclei on the PEDOT surface. Subsequently, these seeds accelerated the water reduction of MnO_4^- and allowed further growth of the MnO_2 domains.[16b,17]

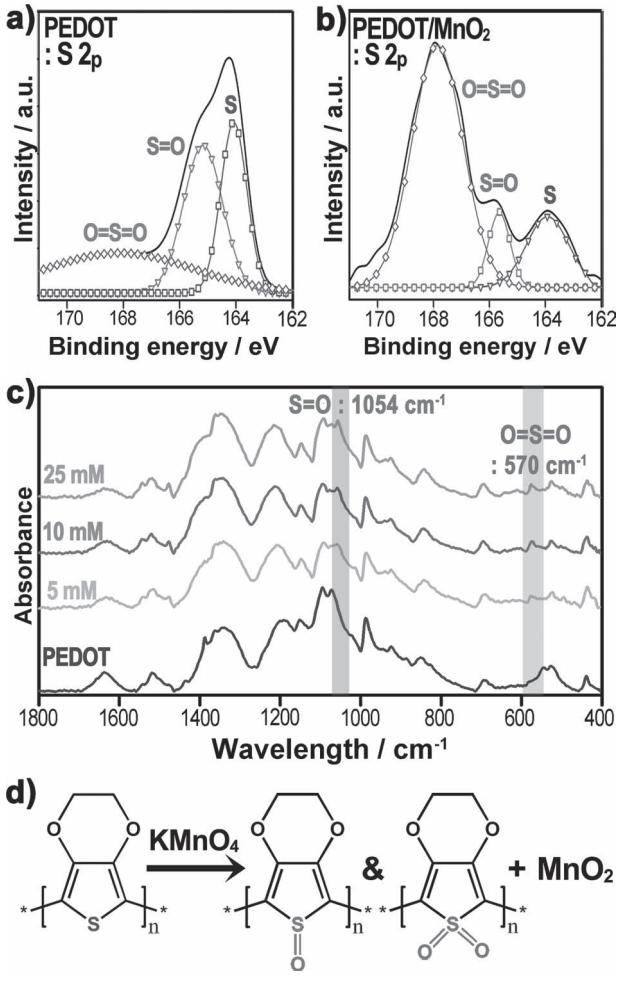

Figure 3. XPS spectra for S 2p of a) PEDOT nanoellipsoids b) after $KMnO_4$ treatment (green, sulfone; red, sulfoxide; blue, sulfide). c) FT-IR spectra of PEDOT and PEDOT nanoellipsoids treated with $KMnO_4$ (5, 10, and 25 mM) for 10 min. d) Proposed mechanism of reduction of PEDOT nanoellipsoids and formation of MnO_2 domains.

Table 1. Atomic percent of Mn, S, and Mn/S ratio of PEDOT/MnO_2 nanoellipsoids with $KMnO_4$ concentration dependance and treatment time dependence. The atomic percent of Mn and S in PEDOT/MnO_2 nanoellipsoids was measured by EDX. Based on these data, the atomic ratio of Mn/S was calculated.

	$KMnO_4$ concentration[a) [mM]			Treatment time[b) [min]			
	5	10	25	5	10	20	25
Mn	4.51	6.20	9.97	5.20	6.20	9.97	12.31
S	4.21	4.75	4.41	4.38	4.75	4.43	4.89
Mn/S	1.07	1.30	2.26	1.18	1.30	2.25	2.87

[a)]The PEDOT nanoellipsoids were treated with 5, 10, and 25 mM of $KMnO_4$ for 10 min; [b)]The PEDOT nanoellipsoids were treated with 10 mM $KMnO_4$ for 5, 10, 20, and 25 min.

2.2. Enhancement of Neurite Outgrowth

To investigate the effect of PEDOT/MnO_2 nanoellipsoids on mammalian neuron differentiation, PC12 cells, derived from the pheochromocytoma of a rat adrenal medulla, were used as a model cell line. These cells sprout neurites and differentiate like sympathetic neuron cells in response to neurotropic molecules, such as NGF.[22] In past decades, MnO_2 nanoparticles have received attention as MRI imaging agents;[23] however, little is known about the influence of MnO_2 nanoparticles on neuronal differentiation. To the best of our knowledge, this is the first investigation of the facilitation of neurite outgrowth by MnO_2 nanoparticles. **Figure 4**a shows immunofluorescent images of PC12 cells treated with NGF and PEDOT/MnO_2 nanoellipsoids and stained with antibodies against β-tubulin (III) (anti-β-tubulin). The β-tubulin (III) is a neuronal-specific intermediate filament protein and so serves as a neuronal marker.[7b] The protein is expressed in PC12 cells when they are exposed to neurotropic molecules, which is the evidence for the differentiation of PC12 cells. The PEDOT/MnO_2 nanoellipsoids facilitated the differentiation of PC12 cells in cooperation with NGF compared with treatment with NGF alone. Morphological changes in the cells were accelerated by increasing the treatment time and concentration of PEDOT/MnO_2 nanoellipsoids. The number of differentiated cells and the average length of neurites also increased in proportion to the dose of PEDOT/MnO_2 nanoellipsoids. Neurite outgrowth was the most obvious when the highest dose of PEDOT/MnO_2 nanoellipsoids was applied to NGF-treated cells at day 3 compared with NGF-treated cells.

Statistical results of the immunofluorescent images were acquired using Image J software (Figure 4b,c). PEDOT/MnO_2 nanoellipsoids affected the cell differentiation efficiency and average neurite length. The number of neurite-bearing cells (cell differentiation efficiency) and their lengths were in proportion to the dose of PEDOT/MnO_2 nanoellipsoids as well as treatment time. At 25 μg mL^{-1} PEDOT/MnO_2 nanoellipsoids for day 1, cell differentiation efficiency and average neurite length were 2 times and 2.3 times higher than those of NGF-treated cells, respectively. In addition, after cells were treated with 25 μg mL^{-1} PEDOT/MnO_2 nanoellipsoids for 3 days, 60% of cells were differentiated and average neurite length was 128 μm. Both data were approximately 1.5 times higher than those of treatment with NGF alone, which represented long-term stimulus to neurite outgrowth. These results indicated that PEDOT/MnO_2 nanoellipsoids gave huge impact on the neuronal

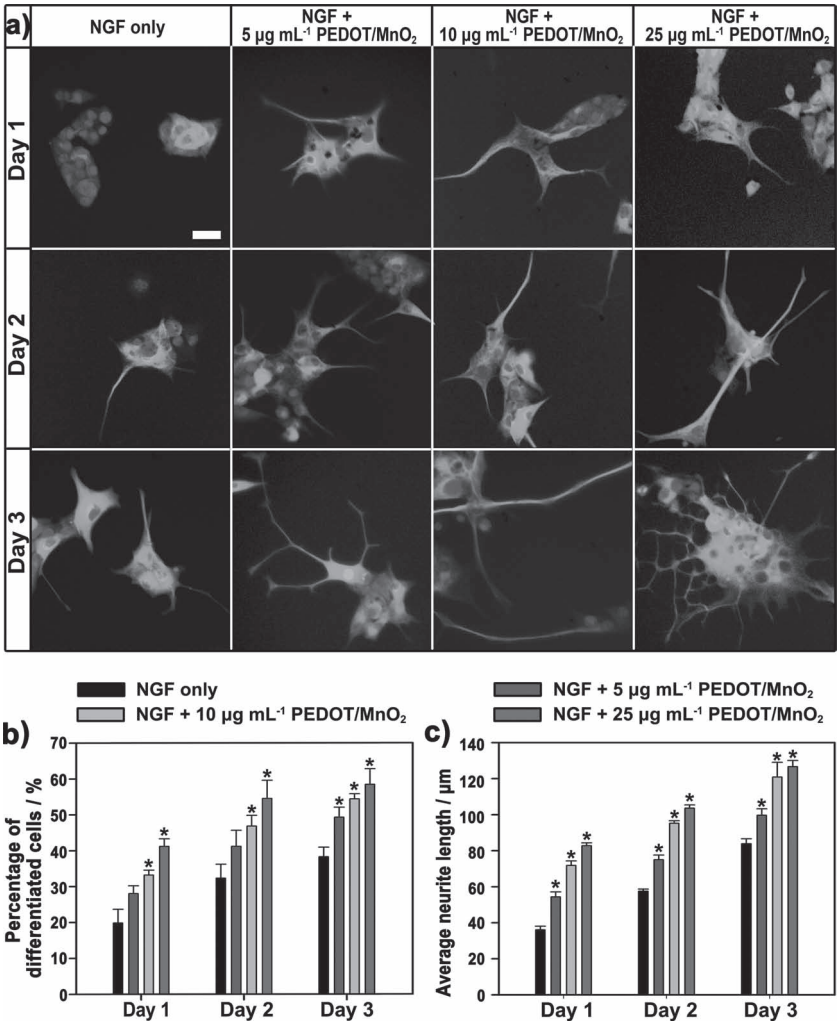

Figure 4. Neuronal response to PEDOT/MnO_2 nanoellipsoids. a) PC12 cells were stained with anti-β-tubulin (class III; neural specific marker; green) and DAPI (nucleus; blue). The cells were incubated with NGF (100 ng mL^{-1}), 0.1% BSA, and different concentrations of PEDOT/MnO_2 nanoellipsoids for 1–3 days (Scale bar: 25 μm). b) Differentiation efficiency of and c) average neurite length of PC12 cells as a function of the dose and time. Values exhibit mean ± SD and independent experiments were performed three times. Neurite-bearing cells and neurite lengths were measured in three random images for each condition ($n = 9$). * denotes a statistically significant difference from the negative control (NGF-treated cell) exposed to the PEDOT/MnO_2 nanoellipsoids ($p < 0.05$).

differentiation not only at early stage of differentiation and but also at mature stage of differentiation.

To compare capability of stimulating neurite outgrowth, control experiments were conducted in PC12 cells (**Figure 5**). In the case of PEDOT/MnO_2 nanoellipsoids without NGF, the cells were not differentiated, indicating that the nanoellipsoids did not activate the differentiation pathway directly, but facilitated the signaling effect when cooperated with NGF (Figure 5a). In case of pristine PEDOT nanoellipsoids and NGF (Figure 5b,e), the cells were differentiated, but no synergetic effect was observed on neurite outgrowth compared with the case of NGF+PEDOT/MnO_2 nanoellipsoids. To investigate the influence of nanostructured MnO_2 toward neurite outgrowth, bulk MnO_2 was treated on the cells (Figure 5c,d). Bulk MnO_2-treated cells and bulk MnO_2+NGF-treated cells showed no extention, mostly damaged shapes, and many floating dead cells due to neurotoxicity of manganase.[24] Considering these data, bulk MnO_2 was harmful to the cells and not effective on neurite outgrowth, but the PEDOT/MnO_2 nanoellipsoids seemed to be safe and effective on differentiation owing to biocompatibility of PEDOT nanoellipsoids.[6b] PEDOT matrix could lead to the internalization of MnO_2 domains and release Mn^{2+} ions inside the cells. The sharp increase in neurite outgrowth is mainly due to an inherent feature of manganese. Roth et al. studied the effects of various divalent metal salts on the morphology of PC12 cells.[5] They found that Mn^{2+} had the greatest facilitation effect on neurite outgrowth compared with other divalent cations at maximal nontoxic concentrations. Furthermore, Mn^{2+} initiated differentiation within several hours after treatment, whereas the process of cell differentiation induced by NGF occurred relatively slowly after several days of treatment.[4,5] Judging from these data, PEDOT/MnO_2 nanoellipsoids with NGF facilitated neurite outgrowth, and the MnO_2 domains played a crucial role in facilitating PC12 differentiation.

Because a small amount of Mn^{2+} was leached from PEDOT/MnO_2 nanoellipsoids in cell culture medium (see Figure 2d), we hypothesized that internalized PEDOT/MnO_2 nanoellipsoids could release Mn^{2+} into the cytosol and activate cell differentiation in cooperation with NGF. To verify this hypothesis, the cellular uptake of PEDOT/MnO_2 nanoellipsoids was visualized by TEM (**Figure 6**a). As displayed in Figure 6a–c, most of the nanoellipsoids were internalized and localized to endosomes (green arrows) and lysosomes (red arrows). PEDOT/MnO_2 nanoellipsoids were

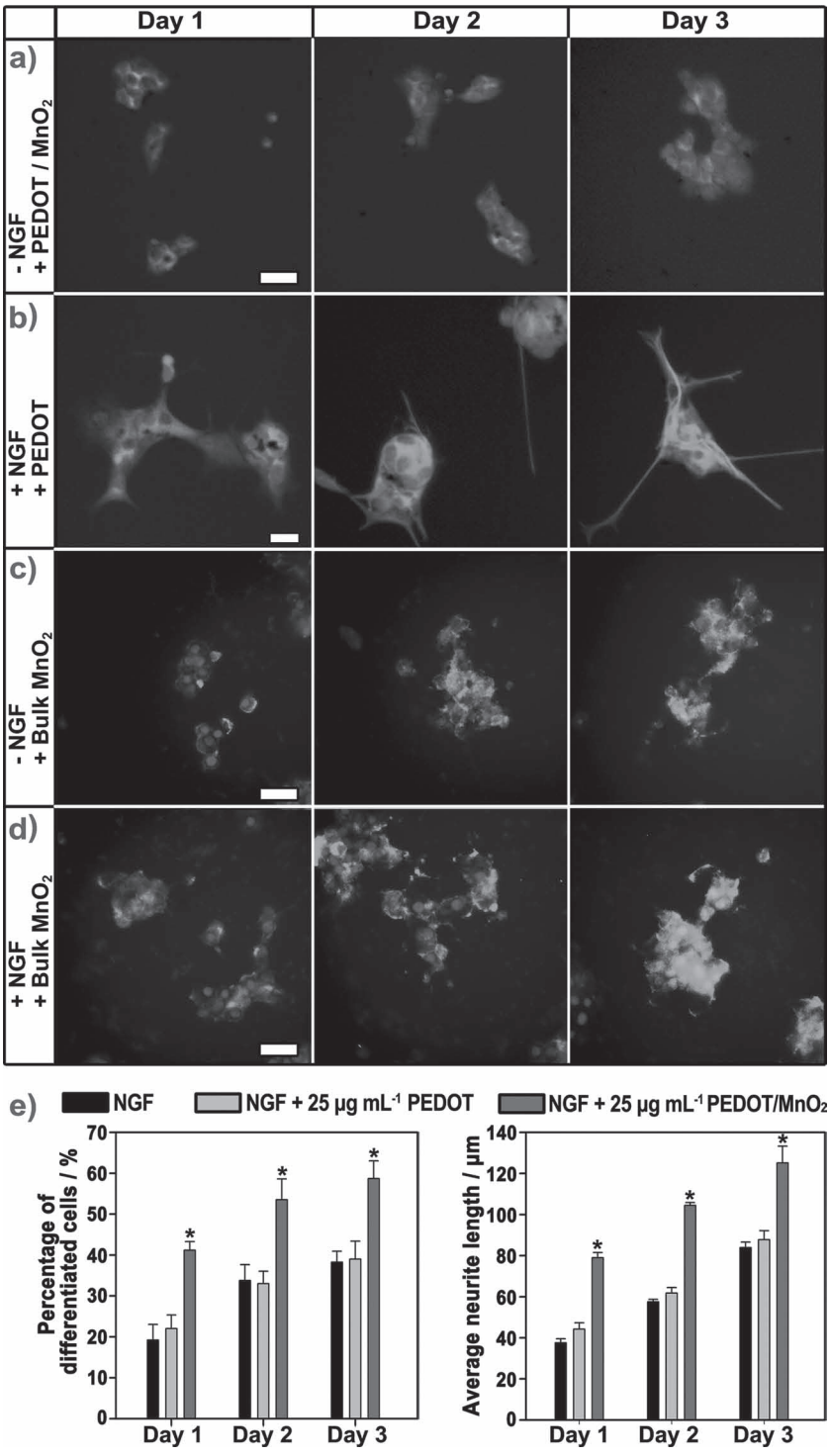

Figure 5. Control experiments as a function of time (1–3 days): a) no NGF and PEDOT/MnO_2 nanoellipsoids, b) NGF+PEDOT nanoellipsoids, c) no NGF and bulk MnO_2, d) NGF+bulk MnO_2, and e) percentage of differentiated PC12 cells and average neurite length of PC12 cells in the presence of NGF, NGF+PEDOT nanoellipsoids, and NGF+PEDOT/MnO_2 nanoellipsoids. These cells were stained with antibodies against β–tubulin III (neural specific marker; green), and DAPI for nucleus (blue). Scale bar: 25 μm. Values exhibit mean ± SD and independent experiments were performed three times and neurite-bearing cells and neurite length were measured in three random images for each condition (n = 9). * denotes a statistically significant difference from the negative control (NGF-treated cells) exposed to the PEDOT nanoellipsoids or PEDOT/MnO_2 nanoellipsoids ($p < 0.05$).

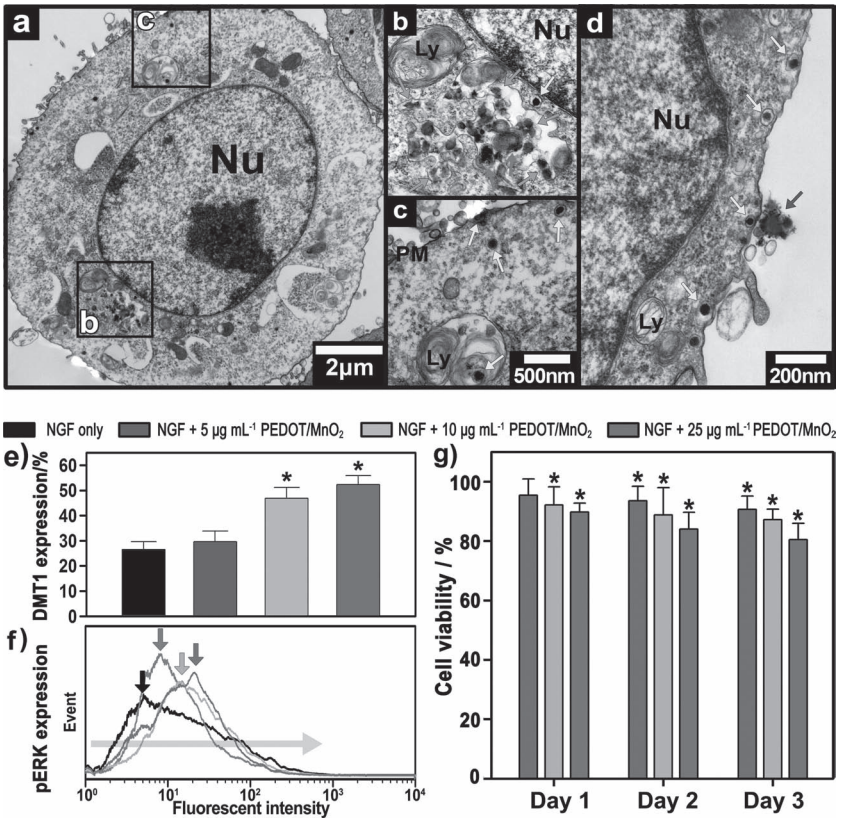

Figure 6. TEM images of PC12 cells incubated with PEDOT/MnO_2 nanoellipsoids (25 μg mL^{-1}) for 24 h. a) Overall PC12 cell morphology and b–d) magnified images. Blue arrow indicates PEDOT/MnO_2 nanoellipsoids seem to be taken up. Green and red arrows denote PEDOT/MnO_2 nanoellipsoids in endosomes and lysosomes, respectively. Yellow arrows show the catecholamines in vesicles. Abbreviations: Nu as nucleus; PM as plasma membrane; Ly as lysosome. e) DMT1 expression and f) pERK expression in PC12 cells treated with NGF and NGF+PEDOT/MnO_2 nanoellipsoids (5, 10, and 25 μg mL^{-1}). The arrows indicated that the apex of the graph. g) Viability of PEDOT/MnO_2 nanoellipsoid-treated PC12 cells with dose dependence (5, 10, and 25 μg mL^{-1}) and time dependence (1–3 days). Values exhibit mean ± SD and independent experiments were performed three times ($n = 3$). * denotes a statistically significant difference from the negative control (NGFtreated cells) exposed to PEDOT/MnO_2 nanoellipsoids ($p < 0.05$).

reached the plasma membrane without aggregation, and they were taken up as a single nanoellipsoid (Figure 6d). In general, the local pH inside the endosomes and lysosomes is pH 5.5–6.3 and pH 4.7, respectively.[25] Under acidic conditions, MnO_2 domains can be partially ionized and released Mn^{2+} ions into the cytosol.[20,26] The MnO_2 domains were still remained on the PEDOT/MnO_2 nanoellipsoids after acidification (Supporting Information Figure S2).

Divalent metal transporter 1 (DMT1) is known as a key protein responsible for the uptake and transport of Mn^{2+} into PC12 cells.[27] DMT1 consists of two isoforms produced by alternate splicing, +IRE and–IRE. Both present at the plasma membrane, the difference in the subcellular localization appears to be dependent upon cation needs. The +IRE and -IRE isoforms are found at the late endosomes/lysosomes and early endosome/recycling endosomes, respectively.[27] The expression level of the DMT1 was quantified using flow cytometric measurement. Figure 6e represented the expression of DMT1 in the PC12 cells incubated with PEDOT/MnO_2 nanoellipsoids and NGF for 1 day. The expression of DMT1 was in proportion of the concentration of PEDOT/MnO_2 nanoellipsoids. In case of 25 μg mL^{-1} PEDOT/MnO_2 nanoellipsoids, the amount of expressed DMT1 increased 2 times higher than that of NGF-treated cells. It is considered that dissolved Mn^{2+} ion from internalized PEDOT/MnO_2 nanoellipsoids affect the expression of DMT1. Transported Mn^{2+} ions using DMT1 activated extracellular-signal-regulated kinases 1/2 (ERK1/2) via phosphorylation.[27] The mitogen-activated protein kinase (MAPK)/ERK signaling cascade is activated by a wide variety of receptors involved in differentiation. ERK1/2, a central component in the MAPK cascade, has been played a role as a major participant in the regulation of cell differentiation. Upon phosphorylation, ERK1/2 moves to the nucleus, and then turns on specific genes initiating cell differentiation and neurite outgrowth. NGF also uses MAPK/ERK signaling pathway.[28] As shown in Figure 6f, the apex of the graph moved to the right, which means the level of phosphorylated ERK1/2 (pERK) increased with an increase in the dose of PEDOT/MnO_2 nanoellipsoids. On the basis of these data, it can conclude that released Mn^{2+} from PEDOT/MnO_2 nanoellipsoids was transported to the mitochondria using DMT1, which activated ERK1/2 pathway in cooperation with NGF. The resulting changes in gene expression cause cell differentiation, which is in good agreement with the above-mentioned hypothesis.[3] However, a high concentration of Mn^{2+} ions within mitochondria not only promoted neurite outgrowth but also acted as a neurotoxin in PC12 cells. Mn^{2+} ion, as a neurotoxin, induce the production of reactive oxygen species (ROS) and lead to disruption of mitochondrial function.[29] Therefore, the viability of PEDOT/MnO_2-treated cells should be further evaluated for biological applications.

The viability of PC12 cells incubated with PEDOT/MnO_2 nanoellipsoids was determined in vitro (Figure 6g). To evaluate the number of viable cells, a highly sensitive luminescence assay was conducted based on the determination of the adenosine triphosphate (ATP) concentration. Cell viability after a 24 h treatment with 25 μg mL^{-1} PEDOT/MnO_2 nanoellipsoids was 91%. After 2 and 3 days, viability dropped to 87% and 81%, respectively. In a previous report, the viability of human fibroblast cells (IMR 90) treated with 25 μg mL^{-1} PEDOT nanoellipsoids was 92% at day 1, and that of PEDOT nanoellipsoid-treated J774A.1 cells was 85%, which indicated no significant effect of MnO_2 domains on viability.[6b] Furthermore, the number of live cells after 3 days was over 80% in the case of 25 μg mL^{-1} PEDOT/MnO_2 nanoellipsoids. These results were comparable with those of other precedent reports.[30] Judging from these results, PEDOT/MnO_2 nanoellipsoids can be considered low toxic materials and are suitable for bio-applications.

2.3. Real-Time Monitoring of Catecholamine Secretion

Due to their biocompatibility and conductivity, PEDOT/MnO_2 nanoellipsoids could be used as a platform for label-free real-time monitoring of catecholamine secretion from PC12 cells. PC12 cells were used as a model to investigate neurotransmitter secretion from neurons as well as to study neuronal differentiation due to process similarity between sympathetic neurons and PC12 cells.[31] Chemical communication between cells is predominantly accomplished by the release of neurotransmitters via an exocytosis' process.[32] Among various chemical messenger molecules, catecholamine molecules (e.g., dopamine, epinephrine, and norepinephrine) are major neurotransmitters. These catecholamines are initially stored in the secretory vesicles with large dense core (Figure 6a–d, yellow arrows).[33] When the intracellular potential increases, the voltage-gated Ca^{2+} channels open following cell depolarization. The influx of Ca^{2+} ions through these channels provokes translocation of secretory vesicles to the plasma membrane. The translocated secretory vesicles fused with the plasma membrane, leading to the release of catecholamines into the extracellular space. In Figure 6c,d, secretory vesicles containing catecholamines can be seen localized near the plasma membrane. Additionally, the release of catecholamines into the extracellular space was also presented in Figure 6c. Once catecholamines were released into the narrow gap between the cell and the PEDOT/MnO_2 nanoellipsoids, they diffused quickly onto the PEDOT/MnO_2 nanoellipsoids and interacted with them by π–π stacking interactions.[34] Interactions between catecholamines and PEDOT/MnO_2 nanoellipsoids affect the charge-carrier density of the PEDOT/MnO_2 nanoellipsoids, and thus allow for label-free monitoring of catecholamine secretion from neurons. A schematic diagram of the system is displayed in **Figure 7**a. The PEDOT/MnO_2 nanoellipsoids were immobilized onto the substrate by vacuum dehydration. This method allows for the delivery of a few nanomaterials into cells, while maintaining most of the nanomaterials immobilized on the substrate.[35]

In order to explore the sensing capability of PEDOT/MnO_2 nanoellipsoids, catecholamines were inserted onto a recording chamber without cells (Figure 7b). All three catecholamines tested induced a sharp current spike due to their aromatic ring, which indicated that the discharge of catecholamines caused a transient increase in the PEDOT/MnO_2 current. High potassium solution and calcimycin, as representative secretagogues, were also introduced into a recording chamber for control experiments. These two molecules, unlike catecholamines, induced a broad and relatively small signal in the absence of cells (**Figure 8**c). Considering these results, PEDOT/MnO_2 sensors were determined to be suitable for label-free real-time monitoring of catecholamine secretion from PC12 cells when secretagogues are introduced.

Figure 8 displays the responses of dopamine, epinephrine, and norepinephrine after gradual addition of catecholamines, increasing their concentration from 0.25 to 2.5 mM. The PEDOT/MnO_2 nanoellipsoids, as a sensor transducer, showed a concentration-dependent increase in current upon exposure to the catecholamines. After removing the catecholamines by washing with 0.1 M PBS, the current returned to its initial level.

PEDOT/MnO_2 nanoellipsoids were used for real-time monitoring of PC12 cells. To investigate the sensor capability

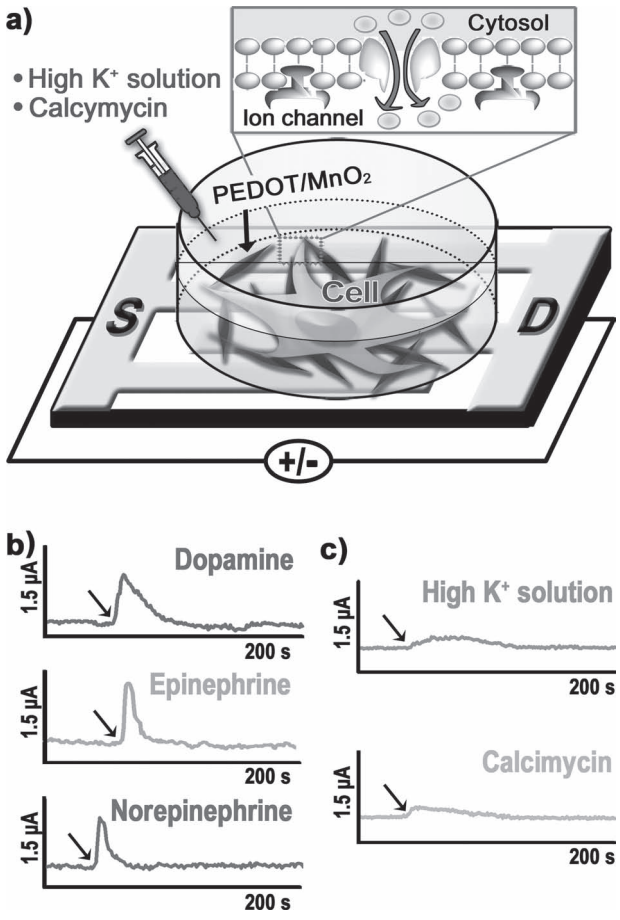

Figure 7. a) A schematic illustration of the experimental setup of sensor application. b) Response of PEDOT/MnO_2 sensor upon exposure of 0.25 mM catecholamines (dopamine, epinephrine, and norepinephrine) and c) response of PEDOT/MnO_2 sensor toward high potassium solution and calcimycin (V_{SD} = 50 mV). The black arrows indicate where the stimulations were applied.

of the PEDOT/MnO_2 materials, the current was monitored in real time at V_{SD} = 50 mV, a low operating voltage. The low V_{SD} is advantageous in terms of minimizing possible disturbances to the living cells and avoiding the instability of devices due to the induced electrochemical or charging effects.[34b] Two secretagogues, high potassium solution and calcimycin, were utilized to induce secretion of catecholamines from PC12 cells. High potassium solution and calcimycin triggered exocytosis via plasma membrane depolarization and formation of Ca^{2+} selective ion channels, respectively. As shown in **Figure 9**, a train of current spikes was detected after the secretagogues were inserted. Each spike corresponded to Ca^{2+}-dependent exocytosis of catecholamines from PC12 cells.[32b,33,34b] The signals generated by these secretagogues can be distinguished from constitutively secreted molecules by their rapid secretion speed. Compared with electrophysiological single-cell recordings,[34c,36] this nanoelectronic approach is non-invasive and does not require high experimental skills.[34a] Therefore, the PEDOT/MnO_2 sensor provides an alternative approach for detecting the dynamic biosensing activities of living cells.

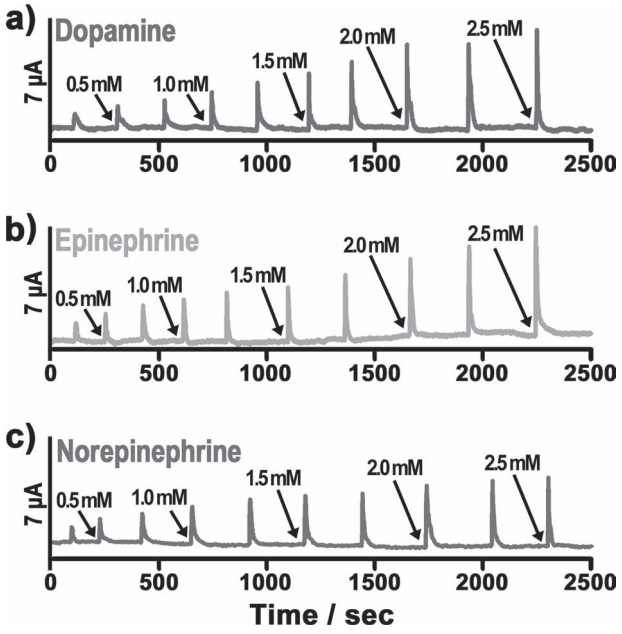

Figure 8. Detection of a) dopamine, b) epinephrine, and c) norepinephrine by PEDOT/MnO_2 sensor (V_{SD} = 50 mV). Each step represents the gradual addition of catecholamines with concentration increasing (0.25, 0.5, 0.75, 1.0, 1.25, 1.5, 1.75, 2.0, 2.25, and 2.5 mM).

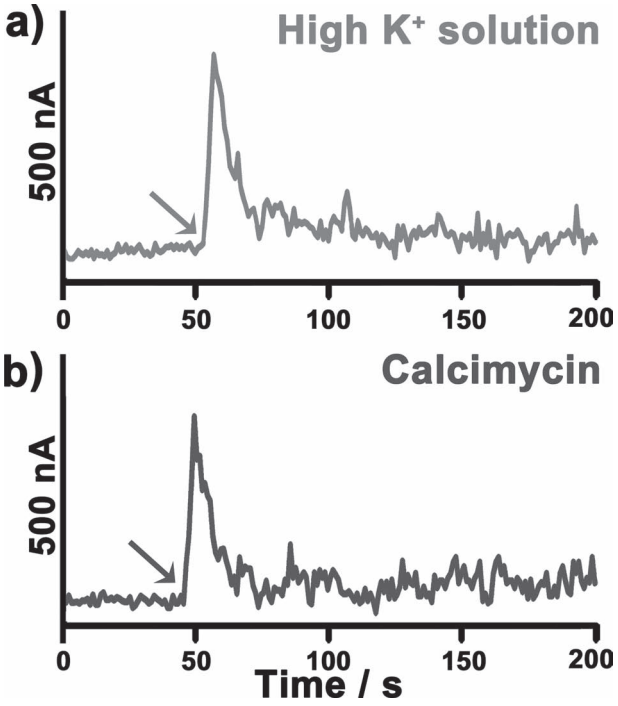

Figure 9. Live cell responses of PEDOT/MnO_2 sensor measured at V_{SD} = 50 mV upon addition of a) high potassium solution and b) calcimycin (arrows signify inserting time).

3. Conclusions

PEDOT nanoellipsoids were fabricated via chemical oxidation polymerization in reverse (water-in-oil) microemulsion and further modified with $KMnO_4$ to form MnO_2 domains on the PEDOT nanoellipsoids by redox deposition. PEDOT/MnO_2 nanoellipsoids were investigated to induce neurite outgrowth during cell differentiation and to enable real-time cellular monitoring of PC12 cells. We systematically examined the morphology, ratio of differentiation, average neurite length, expression level of DMT1, phosphorylation of ERK1/2, viability, and nanoellipsoid uptake of PC12 cells upon exposure to NGF and PEDOT/MnO_2 nanoellipsoids. PC12 cells showed enhanced differentiation with low toxicity in the presence of NGF+PEDOT/MnO_2 nanoellipsoids, where MnO_2 domains played a crucial role in facilitating the differentiation. Moreover, the PEDOT/MnO_2 nanoellipsoids were further applied as transducer for real-time monitoring of PC12 cells. The exocytosis of catecholamines triggered by plasma membrane depolarization and the formation of Ca^{2+} selective ion channels was successfully detected by PEDOT/MnO_2 sensor. The dual-functional PEDOT/MnO_2 nanoellipsoid offers a new method to induce neurite outgrowth and to detect exocytosed biomolecules.

4. Experimental Section

Materials: Sodium bis(2-ethylhexyl) sulfosuccinate (AOT, 98%) was purchased from Aldrich Chemical Co. Ferric chloride ($FeCl_3$, 97%), hexane (99%), and 3,4-ethylenedioxythiophene (EDOT, 98%) were obtained from Aldrich as well. Potassium permanganate ($KMnO_4$) was purchased from Junsei Chemical Co. Catecholamines (dopamine, epinephrine, and norepinephrine), and calcimycin were obtained from Aldrich. All chemicals were used directly without further purification.

Fabrication of PEDOT/MnO_2 Nanoellipsoids: PEDOT nanoellipsoids were fabricated via chemical oxidation polymerization using AOT micelles as the soft template. AOT was dissolved in hexane at a concentration of 3.4×10^{-1} M, and 7 M of aqueous $FeCl_3$ solution was added. The volume ratio of aqueous $FeCl_3$ solution to hexane was 1.1×10^{-2}. All reactions were carried out at 20 °C. The resulting products were thoroughly washed with ethanol to remove residual impurities (residual monomers, surfactants, and oxidizing agents). More detailed experimental procedures and conditions are described in our previous paper.[15] Synthesized PEDOT nanoellipsoids were treated with various concentrations of $KMnO_4$ (5, 10, and 25 mM) under vigorous stirring conditions. PEDOT/MnO_2 nanoellipsoids were formed by reaction between the oxidant and the reductant. Amount of MnO_2 domains depended on the concentration of $KMnO_4$ solution and treatment time. The more MnO_2 domains were loaded in the PEDOT nanoellipsoids, the more cells were differentiated. However, PEDOT nanoellipsoids can be overoxidized by $KMnO_4$ solution (a very powerful oxidizing reagent), which may cause conductivity decrease.[16b] To keep balance between neuronal differentiation efficiency and conductivity for sensor application, PEDOT nanoellipsoids were treated with 10 mM $KMnO_4$ solution for 10 min. The resulting products were thoroughly washed with deionized (DI) water and 0.1 M PBS solution to remove oxidizing agent.

Characterization: Photographs of TEM and HRTEM were acquired with a JEOL JEM-200CX and JEOL JEM-3010, respectively. The amount of MnO_2 domains were investigated using Field Emission Scanning Electron Microscope (FE-SEM, JEOL-6700) equipped with EDX and ICP-MS analysis (JP/ICPS-7500, Shimdzu). The XPS data were obtained with an AXIS-His X-ray photoelectron spectroscopy analyzer (KRATOS). Zeta potential of PEDOT and PEDOT/MnO_2 nanoellipsoids was measured by electrophoretic light scattering with an ELS-8000 instrument (Otsuka Electronics, Japan). FT-IR spectra were recorded on a Bomem MB 100 spectrometer (Quebec, Canada) in absorption modes at a resolution of 4 cm^{-1} and 64 scans. Electrical conductivity was measured by a source-meter at ambient temperature by a four-probe method.

Leaching Profile of the Mn^{2+} Ions from PEDOT/MnO_2 Nanoellipsoids: A leaching profile of the Mn^{2+} ions from PEDOT/MnO_2 nanoellipsoids

was measured in high ionic strength solution (0.1 M PBS) and cell culture medium as a function of a time. PEDOT/MnO_2 nanoellipsoids (5 μg mL^{-1}) were suspended in above mentioned solvents with moderate stirring. Each sample (1 mL) was extracted and centrifuged. The supernatant was transferred to a fresh vial and diluted 5 times with appropriate solvents for ICP-MS analysis (JP/ICPS-7500, Shimdzu).

Cell Culture and Differentiation: Rat pheochromocytoma PC12 cell lines were obtained from American Type Culture Collection (ATCC, Manassas, VA, USA). PC12 cells were cultured in RPMI-1640 medium with 10% horse serum (HS), 5% fetal bovine serum (FBS), 1% penicillin-streptomycin solution, 300 mg L^{-1} L-glutamine, 25 mM sodium bicarbonate, and 25 mM 4-(2-hydroxyethyl)-1-piperazineethane-sulfonic acid (HEPES). Cells were incubated in a 5% CO_2 incubator at 37 °C and 100% humidity. The cells were placed in a 75T flask and maintained at between 1×10^5 and 1×10^6 cells mL^{-1} of medium. The medium was changed every 2–3 days or as required. For differentiation of PC12 cells, cells were seeded (5000 cells cm^{-2}) and incubated for 24 h in serum-reduced medium (1% HS and 0.5% FBS) before treatment with PEDOT/MnO_2 nanoellipsoids. They were added into the medium at concentrations ranging from 5 to 25 μg mL^{-1}. Simultaneously, 100 ng mL^{-1} of NGF (Sigma, St. Louis, MO, USA) and 0.1% bovine serum albumin (BSA) were inserted into the medium to induce the differentiation of PC12 cells. Fresh NGF and BSA were supplied to the medium every two days.

β-Tubulin Imaging: To confirm cell differentiation and measure the neurite outgrowth, cells were stained with anti-β-tubulin. β-tubulin (III), as a neural specific marker, becomes evidence for differentiation of PC12 cells. PEDOT/MnO_2 treated cells were fixed with 4% paraformaldehyde for 10 min, permeabilized with 0.5% Triton X-100 for 5 min, and blocked with 0.1% BSA for 15 min. Then, the cells were stained with Alexa Fluor488 mouse anti-β-tubulin, Class III (neuron specific; BD bioscience, San Jose, CA, USA) for overnight. After rinsing cells with PBS, samples were mounted in Fluoroshield with DAPI (4,6-Diamidino-2-phenylindole dihydrochloride; Sigma, USA). The fluorescent images were obtained by Delta Vision RT imaging system (Applied Precision, Issaquah, WA). To obtain cell images, Cascade II electronmultiplying charge-coupled device (EMCCD) camera was used.

Measurement of Neurite Outgrowth: Neurite outgrowth of PC12 cells was measured in a time- and dose-dependent manner. As described above, PC12 cells were treated with PEDOT/MnO_2 nanoellipsoids, NGF, and BSA for 1–3 days. After incubation, cells were stained with anti-β-tubulin and visualized by Delta Vision RT imaging system. Based on these images, the number of neurite–baring cells and neurite length were calculated using Image J software (National Institute of Health, Bethesda, MD, USA). Neurite-bearing cells were defined as cells with at least one neurite longer than the cell body diameter. The differentiation efficiency was determined by dividing the number of neurite-bearing cells by the total number of cells. The lengths of individual neurites were measured as previously described.[37] Length was defined as the distance from the tip of the neurite to the junction between the cell body and neurite. In the case of branched neurites, the length of the longest branch was measured, and then each branch was measured from the tip of the neurite to the neurite branch point. Average neurite length was calculated by dividing the sum of neurite length by the number of neurite. Independent experiments were performed three times and neurite–bearing cells and average neurite length were measured in three random images for each condition ($n = 9$). More than 100 cells were analyzed in each condition.

Transmission Electron Microscopy: Cellular internalization of PEDOT/MnO_2 nanoellipsoids was observed by TEM. Cells were seed in sterile culture dishes (Nunc, Thermo Fisher Scientific, USA) and incubated for 24 h. Then, the PEDOT/MnO_2 nanoellipsoids (25 μg mL^{-1}), NGF, and BSA were added for another 24 h. After incubation, cells were washed with 0.1 M PBS and collected in eppendorf tubes. Collected cells were prefixed with Karnovsky's fixative containing 2% paraformaldehyde and 2% glutaraldehyde at 4 °C for 2 h. After being washed three times with 0.1 M PBS, the specimen were postfixed with 1% osmium tetraoxide at 4 °C for 2 h and stained with 0.5% uranyl acetate at 4 °C for overnight. Dehydration was conducted through a graded series of ethanol (30, 50, 70, 80, 90, and 100%) and propylene oxide before embedding in spurr's resin. Resin blocks were hardened at 70 °C for 1 day and sectioned by ultramicrotomy. The sections were stained with 2% uranyl acetate and Raynolds' lead citrate and analysis was done using TEM (JEM1010, JEOL, Tokyo, Japan).

Viability Test: The viability of the PEDOT/MnO_2 nanoellipsoid-treated cells was measured using Cell–Titer glow luminescent cell viability assay (Promega, Madison, WI, USA). This assay is a homogeneous method of estimating the number of viable cells based on amount of ATP in metabolically active cells. For the assay, 1.5×10^4 cells mL^{-1} of cells were seeded in white opaque 96-well plates and treated with different concentrations of the PEDOT/MnO_2 nanoellipsoids (5, 10, and 25 μg mL^{-1}), NGF, and BSA for 24 h. After incubation, supernatant was removed and following steps were carried out as supplier's instructions. Cell viability was detected by Victor^3 Multilabel Readers (Perkin Elmer, Boston, MA, USA). The cell viability was determined by dividing the ATP content of NGF+PEDOT/MnO_2 treated cells by the ATP content of negative control (NGF-treated cells).

Immunocytochemistry: As described above, 1.0×10^5 cells mL^{-1} of PC12 cells were treated with PEDOT/MnO_2 nanoellipsoids (5, 10, and 25 μg mL^{-1}), NGF, and BSA for 1 day. After being washed with 0.1 M PBS, the cells were fixed with 4% paraformaldehyde for 20 min, permeabilized with 0.1% Triton X–100 for 15 min, and blocked with blocking solution (0.1 M PBS, 10% FBS, 0.03% 1 M NaN_3) for 30 min. Specific antibodies against phosphorylated ERK1/2 (pERK) and DMT1 (Santa Cruz Biotechnology Inc., Santa Cruz, CA, USA) were diluted with blocking buffer according to the manufacturer's recommendation and incubated with cells for 1 h, respectively. Then, the cells were stained with FITC conjugated secondary antibodies for another 1 h. Cells were washed with 0.1 M PBS and analyzed with flow cytometry (FACS Aria I, BD Bioscience, USA).

PEDOT/MnO_2 Sensor: In order to construct PEDOT/MnO_2 sensor, interdigitated gold electrodes in ECIS chips (8W10E+, Applied Biophysics, Troy, NY) were used as source–drain electrodes. ECIS chip has 8 wells, and each well consists of eight sets of interdigitated gold electrodes (7.5 mm X 0.5 mm, rectangular shape). Cell culture chamber (maximum 600 μL volume, 0.8 cm^2) was designed and used for cell culture–based measurements. For immobilization of PEDOT/MnO_2 nanoellipsoids as a signal transducer, 20 μL of 0.1 M PBS containing 0.1 wt% PEDOT/MnO_2 nanoellipsoids was dropped on the interdigitated electrodes. The PEDOT/MnO_2 nanoellipsoids were immobilized onto the substrate by vacuum dehydration. Then, the source-drain current was monitored when catecholamines were inserted to a recording chamber with a gradual increase in its concentration from 0.25 mM to 2.5 mM (V_{DS} = 50 mV). To detect the dynamic secretion of catecholamines from living cells, PC12 cells (3000 cells) were seed on a chamber of the PEDOT/MnO_2 sensor with 400 μL of serum-reduced medium (1% HS and 0.5% FBS) for 24 h. As described above, PC12 cells were treated with PEDOT/MnO_2 nanoellipsoids, NGF, and BSA for another 24 h. After washing with 0.1 M PBS, cells were treated with calcimycin and high potassium solution (40 mM NaCl, 105 mM KCl, 6 mM $CaCl_2$, 1 mM $MgCl_2$, and 10 mM HEPES).[34b,34c] The source-drain current was monitored at a voltage bias of 50 mV. All electrical measurements were conducted with a Wonatech WBCS 3000 potentiostat.

Supporting Information

Supporting Information is available from the Wiley Online Library or from the author.

Acknowledgements

This research was supported by WCU (World Class University) program through the National Research Foundation of Korea funded by the Ministry of Education, Science and Technology (R31–10013).

Received: August 3, 2012
Revised: October 5, 2012
Published online: November 2, 2012

[1] a) W. C. Lee, C. H. Y. X. Lim, H. Shi, L. A. L. Tang, Y. Wang, C. T. Lim, K. P. Loh, *ACS Nano* **2011**, *5*, 7334; b) T. R. Nayak, H. Andersen, V. S. Makam, C. Khaw, S. Bae, X. Xu, P.-L. R. Ee, J.-H. Ahn, B. H. Hong, G. Pastorin, B. Özyilmaz, *ACS Nano* **2011**, *5*, 4670; c) J. A. Kim, N. Lee, B. H. Kim, W. J. Rhee, S. Yoon, T. Hyeon, T. H. Park, *Biomaterials* **2011**, *32*, 2871.

[2] a) D. S. W. Benoit, S. D. Collins, K. S. Anseth, *Adv. Funct. Mater.* **2007**, *17*, 2085; b) J. M. Razal, M. Kita, A. F. Quigley, E. Kennedy, S. E. Moulton, R. M. I. Kapsa, G. M. Clark, G. G. Wallace, *Adv. Funct. Mater.* **2009**, *19*, 3381; c) X. Shi, S. Chen, J. Zhou, H. Yu, L. Li, H. Wu, *Adv. Funct. Mater.* **2012**, *22*, 3799; d) P.-Y. Wang, L. R. Clements, H. Thissen, A. Jane, W.-B. Tsai, N. H. Voelcker, *Adv. Funct. Mater.* **2012**, *22*, 3414; e) S. L. Wilson, I. Wimpenny, M. Ahearne, S. Rauz, A. J. E. Haj, Y. Yang, *Adv. Funct. Mater.* **2012**, *22*, 3641.

[3] a) K. Kolkova, V. Novitskaya, N. Pedersen, V. Berezin, E. Bock, *J. Neurosci.* **2000**, *20*, 2238; b) S. K. W. Dertinger, X. Jiang, Z. Li, V/ Murthy, G. M. Whitesides, *Proc. Natl. Acad. Sci. USA* **2002**, *99*, 12542; c) Y. Luo, M. S. Shoichet, *Nat. Mater.* **2004**, *3*, 249.

[4] J. A. Roth, C. Horbinski, D. Higgins, P. Lein, M. D. Garrick, *Neurotoxicology* **2002**, *23*, 147.

[5] W. H. Lin, D. Higgins, M. Pacheco, J. Aletta, S. Perini, K. A. Marcucci, J. A. Roth, *J. Neurosci. Res.* **1993**, *34*, 546.

[6] a) S. Kim, W.-K. Oh, Y. S. Jeong, J.-Y. Hong, B.-R. Cho, J.-S. Hahn, J. Jang, *Biomaterials* **2011**, *32*, 2342; b) W.-K. Oh, S. Kim, H. Yoon, J. Jang, *Small* **2010**, *6*, 872; c) W.-K. Oh, S. Kim, M. Choi, C. Kim, Y. S. Jeong, B.-R. Cho, J.-S. Hahn, J. Jang, *ACS Nano* **2010**, *4*, 5301.

[7] a) W. H. Suh, K. S. Suslick, G. D. Stucky, Y. H. Suh, *Prog. Neurobiol.* **2009**, *87*, 133; b) G. A. Silva, *Nat. Rev. Neurosci.* **2006**, *7*, 65.

[8] a) R. A. Green, N. H. Lovell, G. G. Wallace, L. A. Poole-Warren, *Biomaterials* **2008**, *29*, 3393; b) S. M. Richardson-Burns, J. L. Hendricks, B. Foster, L. K. Povlich, D.-H. Kim, D. C. Martin, *Biomaterials* **2007**, *28*, 1539; c) X. Cui, D. C. Martin, *Sens. Actuator B* **2003**, *89*, 92.

[9] D. H. Kim, S. M. Richardson-Burns, J. L. Hendricks, C. Sequera, D. C. Martin, *Adv. Funct. Mater.* **2007**, *17*, 79.

[10] Y.-S. Hsiao, C.-C. Lin, H.-J. Hsieh, S.-M. Tsai, C.-W. Kuo, C.-W. Chu, P. Chen, *Lab Chip* **2011**, *11*.

[11] a) N. A. Kotov, J. O. Winter, I. P. Clements, E. Jan, B. P. Timko, S. Campidelli, S. Pathak, A. Mazzatenta, C. M. Lieber, M. Prato, R. V. Bellamkonda, G. A. Silva, N. W. S. Kam, F. Patolsky, L. Ballerini, *Adv. Mater.* **2009**, *21*, 3970; b) S. F. Cogan, *Annu. Rev. Biomed. Eng.* **2008**, *10*, 275.

[12] a) J. Y. Hong, H. Yoon, J. Jang, *Small* **2010**, *6*, 679; b) J. Jang, J. Ha, S. Kim, *Macromol. Res.* **2007**, *15*, 154.

[13] a) Y. Xiao, C. M. Li, S. Yu, Q. Zhou, V. S. Lee, S. M. Moochhala, *Talanta* **2007**, *72*, 532; b) L. Groenendaal, F. Jonas, D. Freitag, H. Pielartzik, J. R. Reynolds, *Adv. Mater.* **2000**, *12*, 481.

[14] Y. Ner, M. A. Invernale, J. G. Grote, J. A. Stuart, G. A. Sotzing, *Synth. Met.* **2010**, *160*, 351.

[15] a) H. Yoon, M. Chang, J. Jang, *Adv. Funct. Mater.* **2007**, *17*, 431; b) H. Yoon, J.-Y. Hong, J. Jang, *Small* **2007**, *3*, 1774.

[16] a) X. Dong, W. Shen, J. Gu, L. Xiong, Y. Zhu, H. Li, J. Shi, *J. Phys. Chem. B* **2006**, *110*, 6015; b) R. Liu, J. Duay, S. B. Lee, *ACS Nano* **2010**, *4*, 4299.

[17] X. Jin, W. Zhou, S. Zhang, G. Z. Chen, *Small* **2007**, *3*, 1513.

[18] X. Dong, W. Shen, Y. Zhu, L. Xiong, J. Shi, *Adv. Funct. Mater.* **2005**, *15*, 955.

[19] R. Liu, H. Liu, Z. Qiang, J. Qu, G. Li, D. Wang, *J. Colloid Interface Sci.* **2009**, *331*, 275.

[20] T. Xia, M. Kovochich, M. Liong, L. Mädler, B. Gilbert, H. Shi, J. I. Yeh, J. I. Zink, A. E. Nel, *ACS Nano* **2008**, *2*, 2121.

[21] N. B. Patel, D. B. Mistry, *Int. J. Polym. Mater.* **2004**, *53*, 653.

[22] D. G. Drubin, S. C. Feinstein, E. M. Shooter, M. W. Kirschner, *J. Cell. Biol.* **1985**, *101*, 1799.

[23] a) A. A. Gilad, P. Walczak, M. T. McMahon, B. N. Hyon, H. L. Jung, K. An, T. Hyeon, P. C. M. Van Zijl, J. W. M. Bulte, *Magn. Reson. Med.* **2008**, *60*, 1; b) T. Kim, E. Momin, J. Choi, K. Yuan, H. Zaidi, J. Kim, M. Park, N. Lee, M. T. McMahon, A. Quinones-Hinojosa, J. W. M. Bulte, T. Hyeon, A. A. Gilad, *J. Am. Chem. Soc.* **2011**, *133*, 2955; c) J. Shin, R. M. Anisur, M. K. Ko, G. H. Im, J. H. Lee, I. S. Lee, *Angew. Chem. Int. Ed.* **2009**, *48*, 321.

[24] K. M. Erikson, K. Thompson, J. Aschner, M. Aschner, *Pharmacol. Ther.* **2007**, *113*, 369.

[25] a) I. Mallman, R. Fuchs, A. Helenius, *Annu. Rev. Biochem.* **1986**, *55*, 663; b) J. R. Casey, S. Grinstein, J. Orlowski, *Nat. Rev. Mol. Cell Biol.* **2010**, *11*, 50.

[26] a) O. Tsiklauri, T. Marsagishvili, G. Tsurtsumiya, S. Kirillov, D. Dzanashvili, *Russ. J. Electrochem.* **2008**, *44*, 1166; b) E. M. Shapiro, A. P. Koretsky, *Magn. Reson. Med.* **2008**, *60*, 265.

[27] C. Au, A. Benedetto, M. Aschner, *Neurotoxicology* **2008**, *29*, 569.

[28] a) S. Cassano, S. Agnese, V. D'Amato, M. Papale, C. Garbi, P. Castagnola, M. R. Ruocco, I. Castellano, E. De Vendittis, M. Santillo, S. Amente, A. Porcellini, E. V. Avvedimento, *J. Biol. Chem.* **2010**, *285*, 24141; b) M. B. Steketee, S. N. Moysidis, X.-L. Jin, J. E. Weinstein, W. Pita-Thomas, H. B. Raju, S. Iqbal, J. L. Goldberg, *Proc. Natl. Acad. Sci. USA* **2011**, *108*, 19042.

[29] K. M. Erikson, K. Thompson, J. Aschner, M. Aschner, *Pharmacol. Ther.* **2007**, *113*, 369.

[30] a) T.-I. Chao, S. Xiang, J. F. Lipstate, C. Wang, J. Lu, *Adv. Mater.* **2010**, *22*, 3542; b) D. Liu, X. He, K. Wang, C. He, H. Shi, L. Jian, *Bioconjugate Chem.* **2010**, *21*, 1673.

[31] M. S. Qiu, S. H. Green, *Neuron* **1992**, *9*, 705.

[32] a) S. C. Taylor, C. Peers, *J. Neurochem.* **1999**, *73*, 874; b) W. Wang, S. H. Zhang, L. M. Li, Z. L. Wang, J. K. Cheng, W. H. Huang, *Anal. Bioanal. Chem.* **2009**, *394*, 17.

[33] D. M. Omiatek, Y. Dong, M. L. Heien, A. G. Ewing, *ACS Chem. Neurosci.* **2010**, *1*, 234.

[34] a) Y. Liu, X. Dong, P. Chen, *Chem. Soc. Rev.* **2012**; b) Q. He, H. G. Sudibya, Z. Yin, S. Wu, H. Li, F. Boey, W. Huang, P. Chen, H. Zhang, *ACS Nano* **2010**, *4*, 3201; c) H. G. Sudibya, J. Ma, X. Dong, S. Ng, L. J. Li, X. W. Liu, P. Chen, *Angew. Chem. Int. Ed.* **2009**, *48*, 2723.

[35] U. Mittnacht, H. Hartmann, S. Hein, H. Oliveira, M. Dong, A. P. Pêgo, J. Kjems, K. A. Howard, B. Schlosshauer, *Nano Lett.* **2010**, *10*, 3933.

[36] a) T. Cohen-Karni, Q. Qing, Q. Li, Y. Fang, C. M. Lieber, *Nano Lett.* **2010**, *10*, 1098; b) X. Duan, R. Gao, P. Xie, T. Cohen-Karni, Q. Qing, H. S. Choe, B. Tian, X. Jiang, C. M. Lieber, *Nat. Nanotechnol.* **2012**, *7*, 174.

[37] a) N. Gomez, C. E. Schmidt, *J. Biomed. Mater. Res. Part A* **2007**, *81*, 135; b) C. E. Schmidt, V. R. Shastri, J. P. Vacanti, R. Langer, *Proc. Natl. Acad. Sci. USA* **1997**, *94*, 8948.